AIAA JOURNAL
Vol. 33, No. 1, January 1995

Experimental Evaluation of a Box Beam Specifically Tailored for Chordwise Deformation

Lawrence W. Rehfield,* Peter J. Zischka,† Stephen Chang,† and Michael L. Fentress†
University of California, Davis, Davis, California 95616
and
Damodar R. Ambur‡
NASA Langley Research Center, Hampton, Virginia 23692

This paper describes an experimental methodology based upon the use of a flexible sling support and load application system that has been created and utilized to evaluate a box beam that incorporates an elastic tailoring technology. The design technique used here for elastically tailoring the composite box beam structure is to produce exaggerated chordwise camber deformation of substantial magnitude to be of practical use in the new composite aircraft wings. The traditional methods such as a four-point bend test to apply constant bending moment with rigid fixtures inhibit the desired chordwise deformation from occurring, hence the need for the new test method. The experimental results for global camber and spanwise bending compliances correlate well with theoretical predictions based on a beamlike model.

Introduction

STRUCTURAL tailoring concepts have been developed to create wings with elastically produced camber for the purpose of increasing the lift generated by the wing. Currently, the usual means of accomplishing this camber are with controls, the most common of which are flaps. If intrinsic means are used to enhance lift, then flap requirements and their associated systems may be reduced. This new technology will yield weight savings, acquisition cost savings, and maintenance cost savings. The desired effects are illustrated in Fig. 1.

Additional benefits could be realized if this new technology were to be coupled with the Advanced Fighter Technology Integration (AFTI) F-111 wing developed in a joint project between the Air Force Flight Test Center and Boeing Advanced Systems.[1–3] The AFTI program was designed to demonstrate the benefits of a variable camber wing. Among these benefits are 1) enhanced lift, 2) optimum camber for minimum drag, and 3) maximum aerodynamic efficiency over a full modern flight envelope. The AFTI wing consists of deformable continuous surface leading and trailing edges. The camber-producing deformations are created through the use of hydraulic and screw jacks. A blending of an elastically tailored wing box structure and AFTI leading and trailing edges could produce tremendous aerodynamic improvements over the conventional wing structure.

Although it is possible to produce chordwise camber deformation by methods of wing bending and twisting,[4–5] attention will be restricted in the present paper to the method of spanwise bending. This method produces an intentionally exaggerated form of anticlastic curvature that is a natural response to spanwise bending. To use this approach successfully, large effective Poisson ratios need to be created in the wing box while preserving the essential integrity of the wing box cross section.

To test a wing box that produces substantial chordwise elastically tailored deformation when loaded, traditional experimental test methodologies cannot be used. An experimental procedure based upon the use of a flexible four-point bending sling support and load application system (Fig. 2) has been created, and a test was performed on a small-scale box beam model. This new method of four-point loading is described in the present paper, and the results obtained are presented and correlated with theoretical predictions.

Experimental Methodology

The "best" test to perform to evaluate and validate camber production experimentally is a four-point bending test. This test method creates a gauge section in the specimen that is subjected to a pure spanwise bending moment only, a simple state of loading that isolates the desired effect of anticlastic curvature. The challenge, of course, is to create a way of performing the test that utilizes methods of load application and support that permit chordwise camber deformation to occur freely.

Test Specimen Design

The box beam test specimen (Fig. 3) has been designed with the following constraints taken into consideration. The wing box covers are limited to a maximum length of 50.8 cm (20 in.) due to the size of the available composite processing equipment. The cover has a ±26 deg lay-up in keeping with the optimized design without stiffeners.[4] The applied load level has been selected so that measurable strain levels are produced in the covers in the chordwise direction, whereas the load level is below the buckling load of the box beam covers. To prevent the covers from buckling under the four-point bending load, a cover width of 10.2 cm (4 in.) and a 12-ply thickness of 0.191 cm (0.075 in.) has been selected.

Two methods have been used to calculate the buckling load of the box covers, and the results compare well with each other. The covers are made of the Hercules, Inc., AS4/3501-6 graphite-epoxy material system. Typical properties for this material system are presented in Table 1. In the first method, buckling equations for an orthotropic plate with two opposing edges fixed and two opposing edges simply supported were derived. A closed-form solution for a buckling problem with these boundary conditions does not exist, and so the commercially available numerical solution program Theorist[6] was used to solve the buckling equation. This solution yields a buckling load of 4519 N (1016 lb), which in turn relates to a strain level of 1565 μ cm/cm. In the second method, the ratio of the buckling load for a simply supported isotropic plate to that of a fixed-fixed simply supported isotropic plate with the same aspect ratio was determined. This factor was then used to determine the buckling load of the fixed-fixed simply supported orthotropic plate from the buckling load of an orthotropic plate simply supported on all edges. The

Presented as Paper 93-1342 at the AIAA/ASME/ASCE/AHS/ASC 34th Structures, Structural Dynamics, and Materials Conference, La Jolla, CA, April 19–21, 1993; received June 14, 1993; revision received April 8, 1994; accepted for publication April 11, 1994.

*Professor, Department of Mechanical, Aeronautical, and Materials Engineering. Associate Fellow AIAA.
†Graduate Student, Department of Mechanical, Aeronautical, and Materials Engineering. Student Member AIAA.
‡Aerospace Engineer, Aircraft Structures Branch. Senior Member AIAA.

Table 1 Nominal mechanical properties for Hercules, Inc., AS4/3501-6 graphite-epoxy uniderctional tape material

Longitudinal tensile modulus, E_{11}, MN/cm^2	61.3
Transverse tensile modulus, E_{22}, MN/cm^2	5.2
In-plane shear modulus, G_{12}, MN/cm^2	2.6
Major Poisson ratio, ν_{12}	0.30

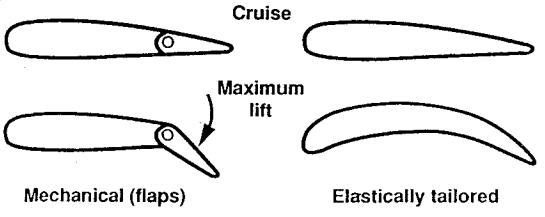

Fig. 1 Methods of increasing airfoil lift.

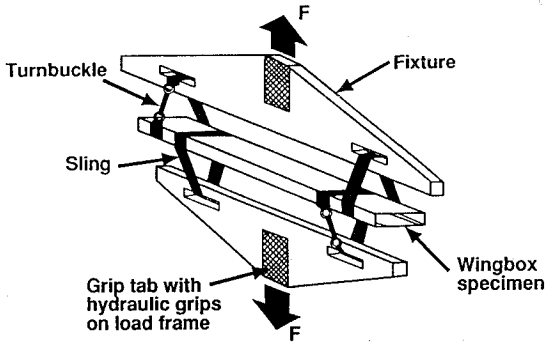

Fig. 2 Overall test configuration.

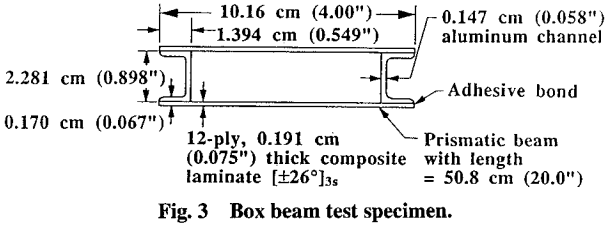

Fig. 3 Box beam test specimen.

resulting buckling load and strain level were 4902 N (1102 lb) and 1701μ cm/cm, respectively. Since these buckling load estimates are conservative, due to the choice of boundary conditions, the cover panel loads during the test were limited to about 2980 N (670 lb).

Experimental Methodology

A number of possible approaches for performing the four-point bending test were devised and thoroughly evaluated. The "sling supported method" was selected for implementation due to its simplicity. An attractive feature of this method is that the entire assembly can be placed in the hydraulic grips of a testing machine and pulled in tension to apply a uniform bending moment to the test specimen. Flexible slings made of nylon strap material are used both to support the test specimen and to apply the four-point loading. This concept seems to provide minimal resistance to the elastically produced camber deformations.

In addition to testing the box beam, a series of component and coupon tests and a detailed finite element analysis of the fixtures were performed. Measured property data on coupon tests were used in the analysis for correlating the test results with theory in the second method of camber correlation, which is discussed subsequently.

All specimen response measurements were made with resistance strain gauges. Although displacement measurements would have been useful, the floating nature of the test setup makes measurement of displacement extremely inconvenient and potentially unreliable. A diagram showing the strain gauge nomenclature and locations appears in Fig. 4. As depicted in the figure, the lengthwise dimension

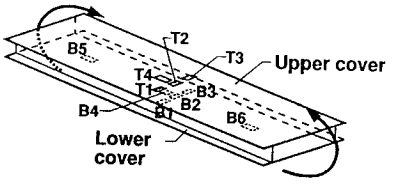

Fig. 4 Strain gauge nomenclature and locations on box beam.

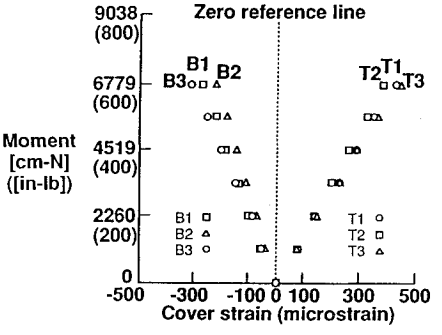

Fig. 5 Bending moment vs chordwise gauge strain.

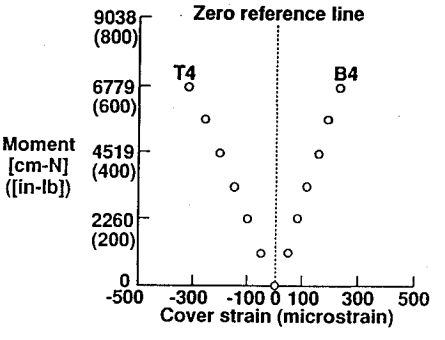

Fig. 6 Bending moment vs spanwise gauge strain.

of the strain gauge measures cover strain in that direction. From these strain gauges we measured spanwise bending strain and chordwise camber strain. The chordwise strain was used to calculate the camber deformations that were produced as a result of the spanwise loading.

Results and Discussion

Basic Strain Gauge Data

Strain gauge data appear in Figs. 5 and 6 as functions of applied bending moment. Data from the chordwise strain gauges are shown in Fig. 5. The zero reference line is provided because, in a theoretically perfect test, the top and bottom gauge readings should be symmetrically located about this reference line. Data from the two spanwise centrally located gauges appear in Fig. 6. Again the zero reference line is provided. Ideally, the two gauges should read the opposite of each other.

Data from the two outer spanwise gauges mounted on the lower cover were used, together with turnbuckle adjustments, to balance the load application system with a small amount of preload. Theoretically, if the test conditions were ideal, the data from these two gauges would be identical, which corresponds to perfect four-point bending conditions.

The previous test results suggest that the objectives of the experiment to generate significant chordwise deformation without box beam cover buckling were met. Several basic relations are needed, however, to interpret the elastic responses associated with structural tailoring from the measured data.

Elementary Mechanics Model

The first relationship involves the spanwise curvature and membrane strains in the box. Let 1 denote the spanwise direction and 2 the normal chordwise direction. If the Bernoulli-Euler assumption, which is valid under pure bending, is adopted, one can write

$$k_{11} = \text{spanwise curvature} = \left(e^l_{11} - e^u_{11}\right)/(H + h) \qquad (1)$$

where e_{11} is the spanwise membrane extensional strain, H is the depth of the box beam, h is the cover panel thickness, and the subscripts l and u denote the lower and upper cover panels of the box beam, respectively.

The second relation provides the elastic law relating spanwise curvature and bending moment. It is given by

$$k_{11} = S_{55}M_y \tag{2}$$

where M_y is the spanwise bending moment, and S_{55} is the spanwise bending compliance given by Ref. 5:

$$S_{55} = (C_{55})^{-1} \tag{3}$$

The spanwise bending stiffness C_{55} can be expressed as

$$C_{55} = 2C_sK_{11}(H/2)^2 + 2(EI)_c \tag{4}$$

In Eq. (4), C_s denotes the structural chord or width of the box beam, $(EI)_c$ is the bending stiffness of the aluminum closure channel shown in Fig. 3 about a chordwise parallel axis, and K_{11} is the spanwise extensional stiffness of the box beam cover panels. For a balanced box beam cover panel configurations and uniaxial stress conditions

$$e_{22} = -(A_{12}/A_{22})e_{11} \tag{5}$$

where A_{12} and A_{22} are the cover panel membrane stiffnesses, and A_{12}/A_{22} represents the effective Poisson ratio.

From classical Bernoulli-Euler bending theory, the chordwise curvature k_{22} is equal to the camber curvature k_c and is given by

$$k_{22} = k_c = (A_{12}/A_{22})/k_{11} \tag{6a}$$

$$= (A_{12}/A_{22})S_{55}M_y \tag{6b}$$

$$= \left(e^u_{22} - e^l_{22}\right)/(H + h) \tag{6c}$$

Equation (6c) is analogous to Eq. (1), and e_{22} is the chordwise membrane extensional strain. Consequently, the camber bending compliance can be defined such that

$$k_c = S_{C5}M_y \tag{7}$$

and the camber bending compliance is

$$S_{C5} = (A_{12}/A_{22})S_{55} \tag{8}$$

Camber Correlation

The most desirable way to correlate results from theory and experiment is to use measured properties of the actual test specimen in the theoretical calculations. This practice is used because there may be a variation in composite structural properties due to variations in processing parameters. For the design and analysis of this experimental wing box, this variation is accounted for by using the material properties for the particular fiber/resin system being used. The purpose here, however, is to evaluate 1) actual vs theoretical elastic camber production, 2) the suitability of the test methodology, and 3) the validity of the analytical model that has been created for use in the design of elastically tailored box beams. With these objectives in mind, the correlation study was conducted in two ways.

The first method is based upon using the experimentally determined spanwise bending compliance as the wing box cover primary elastic characteristic. Using Eqs. (1) and (2), this compliance is readily determined from the plot of experimental spanwise data shown in Fig. 7. The measured spanwise bending compliance S_{55}, together with the theoretical value of the effective Poisson ratio of 1.26 and Eq. (8), permits an estimate of the camber bending compliance S_{c5}. This value of 3.746×10^4 $(\text{N cm}^2)^{-1}$ $[1.075 \times 10^6$ $(\text{lb in.}^2)^{-1}]$ is compared with the experimentally determined value of 3.763×10^4 $(\text{N cm}^2)^{-1}$ $[1.08 \times 10^6$ $(\text{lb in.}^2)^{-1}]$. The experimental value is based upon Eqs. (6c) and (7) and the plot of chordwise strain differential vs moment (Fig. 7).

Although the agreement between analytical and experimental results is excellent, another way of interpreting this information is

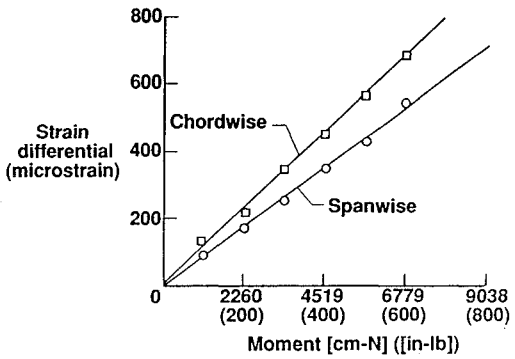

Fig. 7 Strain differential vs moment.

that (A_{12}/A_{22}) can be found experimentally from measured compliances (Fig. 7) and Eq. (8). This interpretation yields an effective Poisson ratio of 1.27, which is in good agreement with the value of 1.26 assumed in the analytical model.

The second method presumes that the box specimen is imperfect. Both the chordwise and spanwise strain gauge data taken during the four-point bending test (Figs. 5 and 6) suggest that a small mean spanwise strain is present. The test was repeated with the specimen position reversed with respect to sling support and loading system. The results were identical compared with the first test. This comparison indicates that the specimen and not the test setup was responsible for the lack of symmetry in the test data about the reference lines.

To understand the reasons for this asymmetry in the test data, a second type of test was conducted on the box beam specimen. The ends of the box were machined to be flat and parallel, and a flat end compression test was conducted with the box positioned between the testing machine platens. Strain gauge data were taken as a function of applied compressive load. These data permitted the extensional stiffness K_{11} and the equivalent imperfection of the specimen to be evaluated.

The imperfect model of the test specimen presumes that bending-extension coupling is present in the box beam specimen. This coupling is due to manufacturing irregularities in the box such as differences in the covers or lack of parallelism of the side closure channels. As a consequence, there is an additional mean extensional strain $\bar{\varepsilon}_{11}$ present in the four-point bending test. This mean strain is evaluated as

$$\bar{\varepsilon}_{11} = \left(e^u_{11} + e^l_{11}\right)/2 \tag{9}$$

With the bending-extension coupling present, strain and curvatures can be written as

$$\bar{\varepsilon}_{11} = S_{11}N + S_{15}M \tag{10a}$$

$$k_{11} = S_{15}N + S_{55}M \tag{10b}$$

In the four-point bending test, the axial force N is zero. Consequently, from Eq. (10a)

$$\bar{\varepsilon}_{11} = S_{15}M \tag{11}$$

A plot of this equation is given in Fig. 8. The bending-extension coupling compliance S_{15}, therefore, is determined from this figure. Note that this compliance is a small negative value -0.045 cm-N^{-1} $(-0.079$ in.-lb$^{-1})$.

In the flat-ended compression test, the box specimen experiences an applied compressive force N_0 and an unknown bending moment. This bending moment corresponds to the compressive load N_0 being applied at a distance e from the central geometric axis. This situation is described by the equations

$$\bar{\varepsilon}_{11} = -(S_{11} + eS_{15})N_0 \tag{12a}$$

$$k_{11} = -(S_{15} + eS_{55})N_0 \tag{12b}$$

Plots of these equations obtained from compression test data are shown in Figs. 9 and 10. With S_{55} and S_{15} previously determined

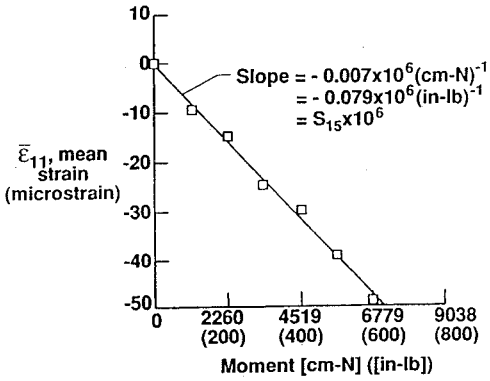

Fig. 8 Average strain vs bending moment—bending test.

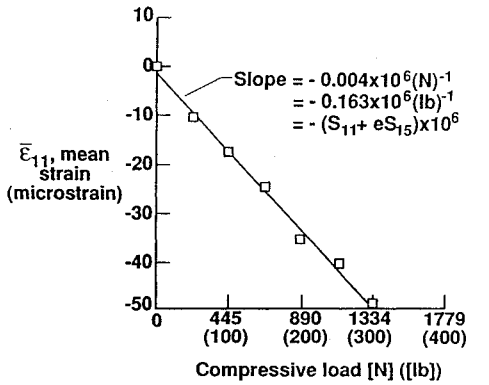

Fig. 9 Average strain vs compressive load—compression test.

from the bending test, extensional compliance S_{11} and the load eccentricity e can be evaluated. The results are $S_{11} = 3.620 \times 10^{-8}\text{N}^{-1}$ ($0.161 \times 10^{-6}\text{lb}^{-1}$) and $e = 0.058$ cm (0.023 in.).

From the elementary rule of mixtures, the box beam stiffness C_{11} is given by

$$C_{11} = 2C_s\bar{K}_{11} + 2(EA)_c \tag{13}$$

The mean cover stiffness is $\bar{K}_{11}$, $(EA)_c$ is the extensional stiffness of the side closure channels, and C_s is the chord length of the wing-section structural box. A coupling parameter γ is now defined as

$$\gamma = (S_{15})^2/S_{11}S_{55} = (C_{15})^2/C_{11}C_{55} \tag{14}$$

The magnitude of this parameter is a convenient measure of the unwanted bending-extension coupling. This parameter has the value 0.046 for the box beam specimen, thus indicating only a small degree of imperfection. The inverse of Eqs. (10a) and (10b) are

$$N = C_{11}\bar{\varepsilon}_{11} + C_{15}k_{11} \tag{15a}$$

$$M = C_{15}\bar{\varepsilon}_{11} + C_{55}k_{11} \tag{15b}$$

where

$$C_{11} = [S_{11}(1-\gamma)]^{-1} \tag{16a}$$

$$C_{15} = -\gamma/S_{15}(1-\gamma) \tag{16b}$$

$$C_{55} = (S_{55})(1-\gamma)^{-1} \tag{16c}$$

The mean cover stiffness is $\bar{K}_{11}$ determined using Eqs. (13) and (16a). The bending stiffness C_{55} is found from Eqs. (16c) and (4).

The correlation of theory and experiment by this second method requires that the coupling parameter γ and the measured mean cover stiffness $\bar{K}_{11}$ of 9.124×10^5 N/cm (0.521×10^6 lb/in.) be used in the theoretical calculations. If this is done, the correlation

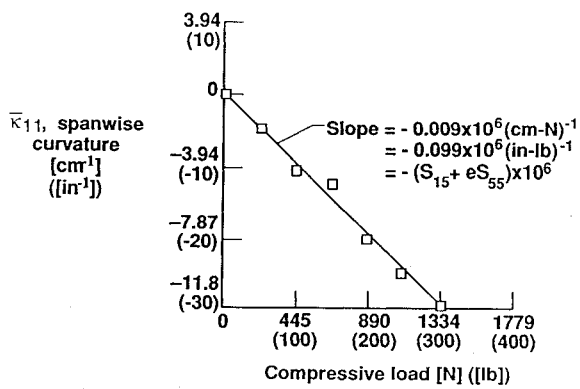

Fig. 10 Curvature vs compressive load—compression test.

of spanwise bending compliance predictions and experimentally determined values can be made. A similar correlation for chordwise camber compliance can also be made. The experimental values for spanwise and camber bending compliances are 2.96×10^{-8} $(\text{N-cm}^2)^{-1}$ [0.85×10^{-6} $(\text{lb-in.}^2)^{-1}$] and 3.76×10^{-8} $(\text{N-cm}^2)^{-1}$ [1.08×10^{-6} $(\text{lb-in.}^2)^{-1}$], respectively. The analytical values of 2.86×10^{-8} $(\text{N-cm}^2)^{-1}$ [0.82×10^{-6} $(\text{lb-in.}^2)^{-1}$] for spanwise compliance and 3.59×10^{-8} $(\text{N-cm}^2)^{-1}$ [1.03×10^{-6} $(\text{lb-in.}^2)^{-1}$] for camber bending compliance show excellent agreement with experimental results.

Concluding Remarks

The unique considerations that are associated with the experimental evaluation of chordwise deformable wing structures are addressed. Since chordwise elastic camber deformations are desired and must be free to develop, traditional experimental methodology cannot be used. An experimental methodology based upon the use of a flexible sling support and load application system has been created and utilized to evaluate a small-scale box beam experimentally.

Experimental data correlate extremely well with design analysis predictions based upon a beamlike model for the global properties of camber compliance and spanwise bending compliance. Local strain measurements exhibit slight departures from theoretical perfection in terms of upper and lower cover asymmetry. This behavior has been explained by accounting for unwanted bending-extension coupling present in the box beam specimen, which was quantitatively evaluated by performing an additional compression test and appropriately analyzing the data.

Since the agreement between finite element simulations, as presented in Appendix C of Ref. 4, and the beamlike predictions is excellent, and the correlation with experiments is very good as explained in the present paper, the design of chordwise-deformable wings by utilizing the bending method of producing camber is valid.

References

[1]Scott, W. B., "Performance Gains Confirmed in Mission Adaptive Wing Test," *Aviation Week & Space Technology*, Oct. 3, 1988, p. 77.

[2]Smith, S. B., and Nelson, D. W., "Determination of the Aerodynamic Characteristics of the Mission Adaptive Wing," *Journal of Aircraft*, Vol. 27, No. 11, 1990, pp. 950–958.

[3]Smith, S. B., and Bonrome, K. L., "AFTI/F-111 Mission Adaptive Wing Flight Research Program," *AIAA Fourth Flight Test Conference*, AIAA, Washington, DC, 1988, pp. 155–161 (AIAA Paper 88-2118).

[4]Rehfield, L. W., Chang, S., and Zischka, P. J., "Modeling and Analysis Methodology for Aeroelastically Tailored Chordwise Deformable Wings." NASA CR-189620, July 1992.

[5]Rehfield, L. W., "Design Analysis Methodology for Composite Rotor Blades," *Proceedings of the Seventh DoD/NASA Conference on Fibrous Composites in Structural Design*, Air Force Wright Aeronautical Lab., AFWAL-TR-85-3094, Wright-Patterson AFB, OH, June 1985, pp. (V(a)-1)–(V(a)-15).

[6]Anon., *Theorist Reference Manual*, second printing, Prescience Corp., San Francisco, CA, 1991.